AGH Journal of Mining and Geoengineering • Vol. 36 • No. 2 • 2012

*Grzegorz Lizurek *, Stanisław Lasocki **

STUDIES OF INDUCED SEISMIC EVENTS CLUSTERING IN EQUIVALENT DIMENSION SPACES IN CHOSEN RUDNA MINE PANELS

1. Introduction

The induced seicmicity in the Legnica–Glogow Copper District (LGCD) located in Lower Silesia SW Poland is connected with three copper mines: Lubin, Polkowice-Sieroszowice and Rudna, which exploit the copper ore. Annually, local seismic networks record several hundred events with a local magnitude range of between 0.4 to 4.5. Some of the seismic events induced by mining operations are rockbursts, which can cause fatalities and injuries among the miners. These strong events induced by mining operations are able to cause ground motion felt on the surface and affect surface installations in the area above the mines. The highest peak of ground acceleration caused by the strongest mining induced events recorded in the LGDC area exceeded 2.0 $m \cdot s^{-2}$ [13].

The generation process of mining induced seismic events depends on complex and time–variable anthropogenic and natural factors. Studies of mining induced seimicity confirmed that in Polish mines events connected directly with mining operations and events connected with large discontinuities can be distinguished [1, 3, 5, 8, 9]. Complex and mulitmodal magnitude distribution is a result of the above mentioned feature [12]. The parameters of mining induced seismicity are in general time-dependent, and the processes often have a memory [11, 14]. Studies of the temporal and spatial patterns of mining induced seismicity provided the evidence for interrelations of seismic events [2, 7, 18, 19, 22, 23].

In this paper the temporal changes of seismic event parameters are investigated. The study aim was to find out whether the temporal clustering of smaller events in different parameters can be observed before and after high energy events ($M_l \geq 3$) from different mining panels. The method chosen for the analysis was the study of the temporal variation of the frac-

* Institute of Geophysics, Polish Academy of Sciences, Warszawa

tal dimension of the seismic events parameters — the interevent epicentral distance (*dr*), the interevent time (*dt*), logarithm of seismic energy (*lE*) and interevent energy coefficient (*dlE*), which is the absolute difference between the logarithms of the energy of two consecutive events. The transformation of the seismic source parameters into equivalent dimension (*ED*) space was done before the temporal behavior studies. The transformation allowed for the estimation of the fractal dimension of the different parameters using the same method — correlation fractal dimension, and then easily compare the obtained temporal changes of the fractal dimensions of different parameters. The effect of the grouping is expressed by a decrease of the fractal dimension, which is connected with the similarity of the events parameter values. The temporal changes of the fractal dimension of seismicity before the strongly induced events would indicate some initiation phase of the process leading to a high energy release.

2. Rudna Copper Mine: mining panels and seicmicity

Mining induced seimicity in the Rudna Copper Mine was also considered in this study. The mine is located in Legnica-Glogow (Lubin) Copper District, in the Southwestern part of Poland. The ore bearing strata is included in a Permian series of dolomite, shale and sandstone layers, above them is the evaporate series composed of anhydrite and salt layers. The approximate depth of the ore bearing layers is between 900–1100 meters. Below the copper ore strata lies Rotliegend sandstone. The exploitation is performed in several mining panels. The mining works in this mine are performed in the "pillar–chamber" regime. Blasting is the method used for extracting the copper ore due to its hardness (15–170 MPa). The ore seam is comprising of 3 types of rock: dolomite and sandstone, separated by a main layer of copper-bearing shale [6]. The events chosen for analysis were located near front of the excavation in a considered time period. Those events are assumed to be connected directly with the exploitation regime.

The seismicity in Rudna mine is monitored continuously with local underground seismic network, which is composed of 32 vertical seismometers at mining level, except 5 sensors placed in elevator shafts. The depth of the seismometers varies from 300 down to 1000 meters below the surface. Epicenter location accuracy is about 50 m [16]. A catalog of 621 mine induced events of energy from $1.3 \cdot 10^3$ J to $1.2 \cdot 10^8$ J (local magnitude from 1 to 3.5) from three different mining panels: G-11/8 (183 events), G-7/5 (125 events), XVII/1 (313 events) from 2004 to 2010 recorded by Rudna Copper Mine seismological network was then analyzed. The focal mechanism of every studied high energy event was determined with moment tensor inversion method [24]. The completeness level varies according to the mining area, but the whole mining catalog has a completeness level at $M_L = 1.2$. All of the studied high energy events are named with a panel code. In the case of panels with more such events, the respective number is added according to the order of the high energy event occurrence in studied panel.

The first studied case were 125 events from the G-7/5 mining panel. The high energetic events were 2009-07-21 from here on called the event G7/5-1. Its energy was $9.3 \cdot 10^7$ J and local magnitude was 3.5. The stronger second event in this panel, the event G7/5-2 occurred on 2010-02-20. Its energy was $1.2 \cdot 10^8$ J, and $M_L = 3.5$. The completeness level for the data from the

G7/5 mining panel was M_L = 1.3. The considered time period was from 2008-07-03 to 2010-03-25. The spatial distribution of the studied events in the G7/5 mining panel is shown in figure 1.

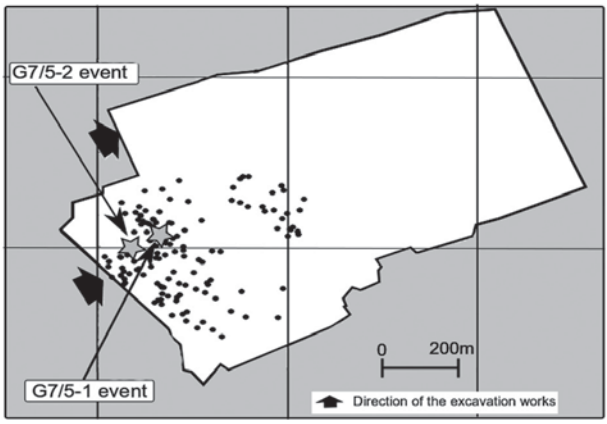

Fig. 1. Spatial distribution of seismic events in G7/5 mining panel, white area is the mining field, black dots are the studied event epicenters

Seismic activity was calculated for 40 event windows being shifted in one event. The seismic activity varied from 0.16 to 0.33 events per day (Fig. 2). The highest activity was at the end of studied period, the increase of activity can be observed before the second high energy event: G7/5-2. The increase of activity was not observed before a first studied event (G7/5-1 event), which was followed by a rockburst. For both of the events, vertical location was at the excavation level in the dolomite copper ore bearing strata. The focal mechanism of the G7/5-1 event was mostly double-couple. The G7/5-2 event from this panel was provoked by blast works. The solution mechanism was different than in the above case of the G7/5-1 event. The G7/5-2 event had a large non double couple component mechanism (above 80%). The interpretation of the mechanism is in the uniaxial pressure of the above lying rockmass, causing the rockmass to collapse under its own weight. The strike of the nodal planes of both events are nearly parallel to the directions of the observed in the G7/5 mining panel tectonic faults of the NW-SE and SW-NE direction. Also observed are similarly orientated cracks of a couple of centimeters width filled in with gypsum, calcite, anhydrite and clay minerals.

The next event studied was from the G-11/8 panel from 2008-09-06 with an energy of $2{,}3 \cdot 10^7$ J, M_L = 3.2 — G11 during the event. The time period chosen for the clustering studies was from 2008-04-02 to 2008-12-28 with 183 events, the data completeness level in this mining area was M_L = 1.2. The spatial distribution of the events within mining panel is presented in figure 3.

The activity in the considered time period estimated for the 40 events in the moving window varied from 0.4 to 1.5 event per day (Fig. 2). Activity was the highest in the first half of the considered period, then gradually decreased. After the G11 event from 2008-09-06 the activity in the panel decreased further reaching the lowest values. The focal mechanism of the event shows a high non double couple components (about 90 % of the mechanism). With

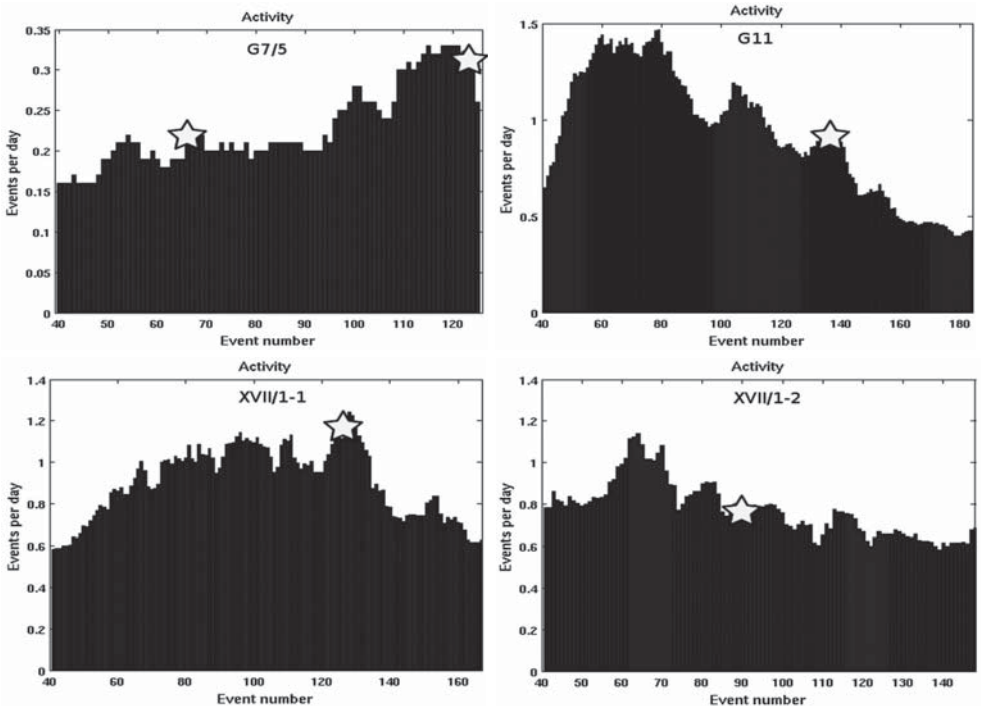

Fig. 2. Activity in studied mining panels estimated for the 40 event moving windows. Bars are representing number of events per day, stars are the high energetic events respectively: upper left panel — G-7/5 -1, G-7/5-2, upper right panel — G11, lower left panel — XVII/1-1, lower right panel — XVII/1-2

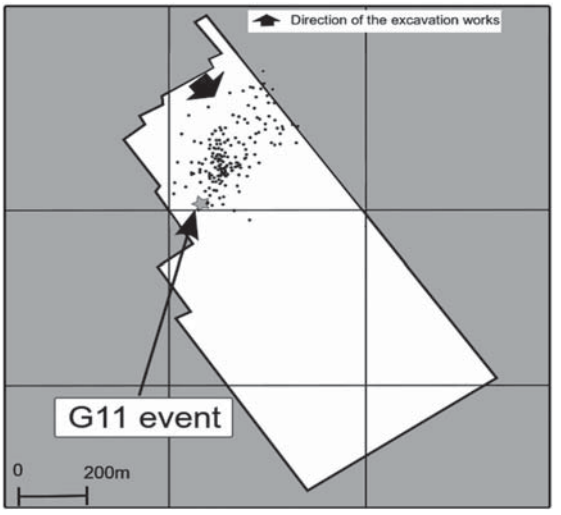

Fig. 3. Spatial distribution of seismic events in G11/8 mining panel, white area is the mining field, black dots are the studied event epicenters

the nodal plane strike (40,5° A plane or 211,6° B plane) similar or perpendicular to the main crack direction in the surrounding rock mass, which was 35° and 315° NE-SW and NW-SE. There were no tectonic faults observed in the mining panel. The events spatial location and depth were determined by the Rudna Mine. According to a depth (h = –914m) the event took place above the roof of the mining level in the anhydrite strata.

The next events analyzed in this study were from the XVII/1 mining panel. The first analyzed event was from 2008-06-17 with an energy of $2.6 \cdot 10^7$ J, M_L = 3.2 (XVII-1 event), the considered period of the seismic activity in this mining panel covered an interval between 2008-01-14 and 2008-08-20 with 166 events. The completeness level of the XVII mining panel catalog was M_L = 1. The activity estimated for the 40 events in the moving window varied from 0.6 to 1.2 event per day (Fig. 2). The activity was lower (about 0.6 events per day) during the early period of the considered time span, then an increase in activity was observed reaching a maximum shortly after the XVII-1 event. After the considered event, activity started to decrease. The event was located in a strata lying above the mining level — anhydrite strata.

The focal mechanism of the XVII-1 event was mostly non double couple, with only 43% of the double couple component in mechanism solution. The direction of one of the nodal planes was similar to that observed in the NW–SE faults and the main cracks in the mining panel.

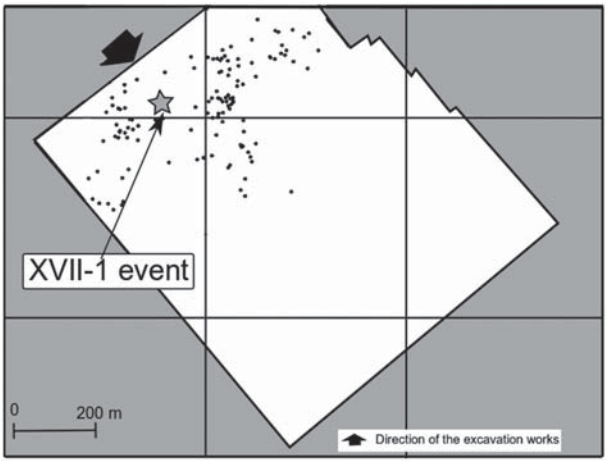

Fig. 4. Spatial distribution of seismic events in XVII mining panel, white area is the mining field, black dots are the studied event epicenters

The last of the analyzed events was the $E = 1.1 \cdot 10^7$ J, M_L = 3 event (XVII-2 event) from 2009-07-06. The time period chosen for the analysis was from 2009-03-13 to 2009-09-30, and during this period 147 events took place. The completeness level of the XVII mining panel catalog was M_L = 1. Seismic activity in this period was varying in time from 0.6 to 1.2 event per day (Fig. 2). The highest point of activity was in first part of the considered period but not directly before the biggest event. This event was also located in a anhydrite strata approximately 180 meters above the ore bearing layer. The focal mechanism of this event was mostly double

couple with about 35% of non double couple components. The nodal planes determined in focal mechanism solution are different than the observed directions of the main faults in the area of the XVII panel. The direction of the faults observed are NW–SE or NE–SW (approximately the same as the main observed crack directions), and the determined nodal planes are rotated about 45 degrees anticlockwise against the observed direction of faults.

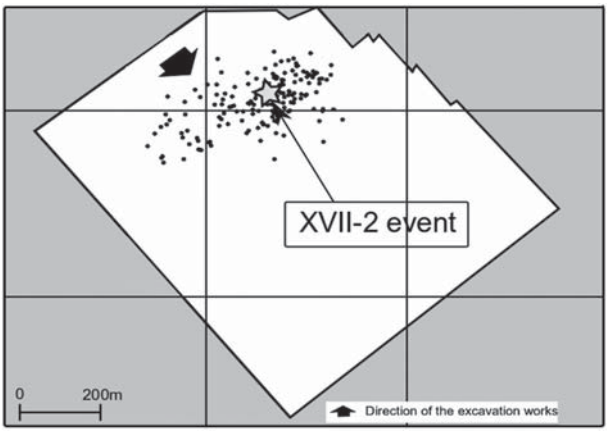

Fig. 5. Spatial distribution of seismic events in XVII mining panel, white area is the mining field, black dots are the studied event epicenters

3. Method of analysis

The temporal changes of the seismic event parameters were the main subject of the study, which aimed to check if the temporal clustering of smaller events in different parameters can be observed before and after the high energy events ($M_l \geq 3$) in different mining panels.

The mining induced seismic events are parameterized for the purpose of this study by the origin time (*t*), the epicentral coordinates (*x*, *y*), the interevent epicentral distance (*dr*), the interevent time (*dt*), logarithm of seismic energy (*lE*) and the interevent energy coefficient (*dlE*). The interevent distance (*dr*) is the epicentral distance between two consecutive events in catalog. The interevent time (*dt*) is the time interval between the two consecutive events. The interevent energy coefficient (*dlE*) is the absolute difference between the logarithm of energy of the two consecutive events. The temporal changes of the fractal dimension of the seismic events parameters — the interevent epicentral distance (*dr*), the interevent time (*dt*), logarithm of seismic energy (*lE*) and interevent energy coefficient (*dlE*) was the method chosen for analysis. The fractal dimension was calculated with the correlation fractal dimension method proposed by [4].

The distribution of the parameters chosen for the study may be different, therefore the analysis of the temporal behavior of the fractal dimension in is space composed of such differently distributed parameters that it may be misleading. The transformation of the differently distributed parameters into equivalent dimension (*ED*) space allowed for the estimation of the fractal dimensions using the same method (fractal correlation dimension) and then

compare the obtained temporal changes of the fractal dimension of the different parameters, that may be differently distributed before the transformation. Details of the method can be found in [15, 17]. The effect of the clustering is expressed by a decrease of the fractal dimension, which is connected with the similarity of events parameter values. The temporal changes of the fractal dimension of seismicity before the strongly induced events would indicate some initiation phase of the process leading to the high energy release. The transformation of the seismic source parameters into *ED* space was carried out before the temporal behavior studies.

The long-term distribution of every considered event parameter in equivalent dimension is uniform in [0,1]. The degree of the uniformity of the distribution of points in ED space was quantified with a fractal dimension. If this distribution was uniform then the fractal dimension equals the number of the dimensions of the *ED* space.

Data from every panel was transformed separately into equivalent dimensions. The long term basis of the transformation were: 125 events from G-7/5 mining panel from 2008-07-03 to 2010-03-25 in case of G7/5-1 and G7/5-2 events, 183 events from G-11/8 from 2008-04-02 to 2008-12-28 in case of G11 event, 166 events 2008-01-14 and 2008-08-20 in case of XVII/1-1 event and 147 events from 2009-03-13 to 2009-09-30 in case of XVII/1-2 event. A fractal dimension analysis was performed on the *ED* space representations of the events for single parameters. The temporal variations of then event clustering was studied by calculation of the fractal correlation dimension in a 40 event length moving window. The step of the window was one event. Hence, the starting window was composed of the first 40 events from the considered catalog, the next window had 39 events in common with the previous one. The study was performed for five chosen high energy events ($E > 10^7$ J). Before and after chosen events no other comparably strong events took place within a temporal window span, therefore the observed temporal changes were considered as a representation of the seismogenic process connected with the studied event and the process of the studied event was not influenced by other high energy events from the same mining area. Other influences on the temporal variation were limited to mining excavation works.

Changes in the fractal dimension indicated the changes in the concentration of the event locations in considered one dimensional *ED* space. If the fractal dimension was getting lower, then the events tended to cluster in space, for instance in uniformly distributed events in one dimensional space the fractal dimension of the events were $r \approx 1$, but when the events were grouped in a cluster then the fractal dimension was lower. The fractal dimension was estimated for all of the studied catalogs separately. All events in the considered mining panel, all in dimensional *ED* spaces were always approximately 1 ± 0.01.

4. Results

The temporal changes of the fractal dimension were calculated separately in different ED parameters (*dt*, *dr*, *dlE* and *lE*). The results of the temporal variation of the fractal dimension of the *dt*, *dr*, *dlE* and *lE* for all of the considered events are shown in figures 6, 7, 8 and 9 respectively.

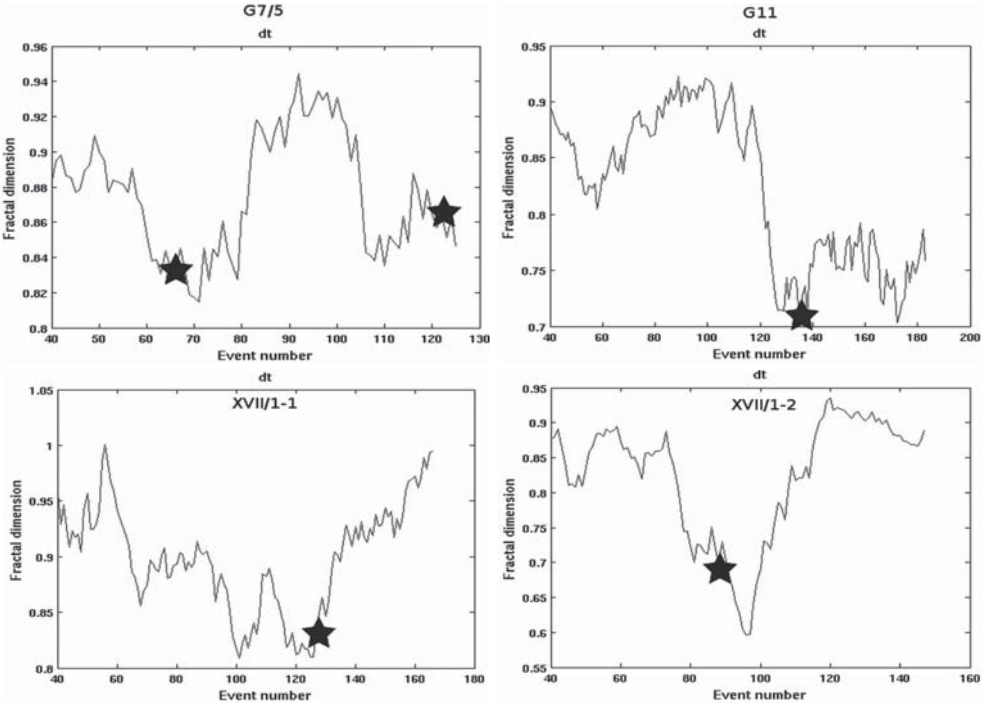

Fig. 6. Temporal changes of fractal correlation dimension of dt parameter. The solid line represents the fractal correlation dimension and stars are the high energetic events: G7/5-1, G7/5-2 (upper left panel), G11 (upper right panel), XVII/1-1 (lower left panel), XVII/1-2 (lower right panel)

The amplitudes of the fractal dimension variations of all parameters, with the exception of one case, are similar and the value of maximum amplitude varies between 0.15 and 0.3. The one exception is the highest amplitude observed in the case of the temporal fractal dimension variation of dr parameter, the maximum amplitude is around 0.45 in case of XVII/1-1 event.

The lowering of the fractal dimension of the *dt* parameter, before the all high energetic events and increase of the fractal dimension, after all high energetic events is visible in figure 6, except in the case of the G7/5-2 event, which is at the end of the catalog. The magnitude and character of changes differ — in the case of the G11 event, there is sudden drop of fractal dimension several samples before the G11 event, and the magnitude of this drop is 0.18, while in other cases, the decrease before the high energy event starts earlier. The magnitudes of the G7/5-1 and the G7/5-2 events are similar and about 0.1. The decrease of fractal dimension of dt parameter began approximately 20 events before the high energy events from this mining panel. The magnitude of the temporal changes in the fractal dimension of the *dt* parameter in the case of XVII/1-1 and XVII/1-2 are similar (0.18 and 0.2 respectively), but the decrease in the fractal dimension before the XVII/1-1 event started much earlier (about 60 events before the main event) with the main drop between the 60th and 70th event in the catalog (drop magnitude 0.15) then slightly rose and after another 20 events, again with drops of about a 0.1 magnitude one final increase happened. About 20 events before the XVII/1-1

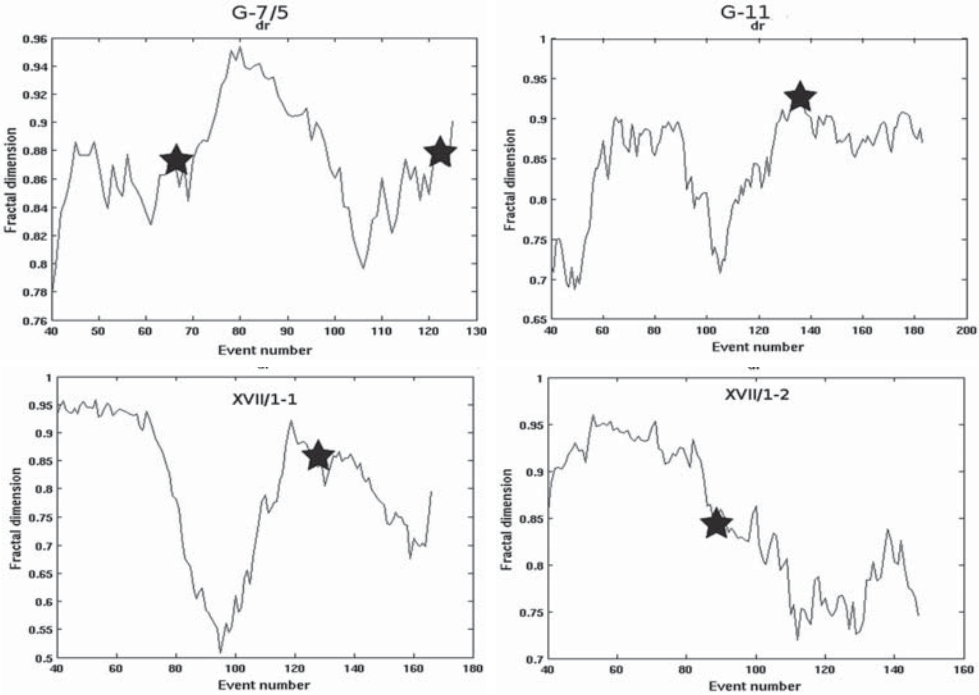

Fig. 7. The temporal changes of the fractal correlation dimension of dr parameter. The solid line represents the fractal correlation dimension and stars are the high energetic events: G7/5-1, G7/5-2 (upper left panel), G11 (upper right panel), XVII/1-1 (lower left panel), XVII/1-2 (lower right panel)

event fractal dimension of the *dt* parameter drops which took place for the last time (the drop magnitude was about 0.06). The decrease in the fractal dimension started about 20 events before the XVII/1-2 event, then after the event, the decrease continued for about 15 events and then an increase in the fractal dimension started.

The temporal behavior of the fractal dimension of the *dr* parameter is similar in the XVII/1-1, G-11 and G7/5-2 events (Fig. 7). A decrease in the fractal dimension of the *dr* parameter to a local minimum (amplitude of decrease: 0.45, 0.2 and 0.24 respectively for XVII/1-1, G-11 and G7/5-2 events), was then followed by on increase, after which the event happened. The decrease in the fractal dimension started in all three cases about 40 events before the main one. In the case of the G7/5-1 event, there was a 0.1 magnitude increase in the fractal dimension of the *dr* parameter after the event. About 30 samples before this event a 0.1 magnitude increase in the fractal dimension is visible. The fractal dimension of the temporal changes in the *dr* parameter of the XVII/1-2 event series shows a decrease in the fractal dimension value (0.1 magnitude of decrease), which started 15–20 samples before the main event, but after the XVII/1-2 event a decrease (0.13 magnitude of decrease) continued, and after 30 samples reached a minimum.

The temporal variations of the *dlE* parameters in all of the studied cases, reached a maximum of amplitude changes between 0.17 to 0.28 (Fig. 8). Before the G7/5-1, G11, XVII/1-1

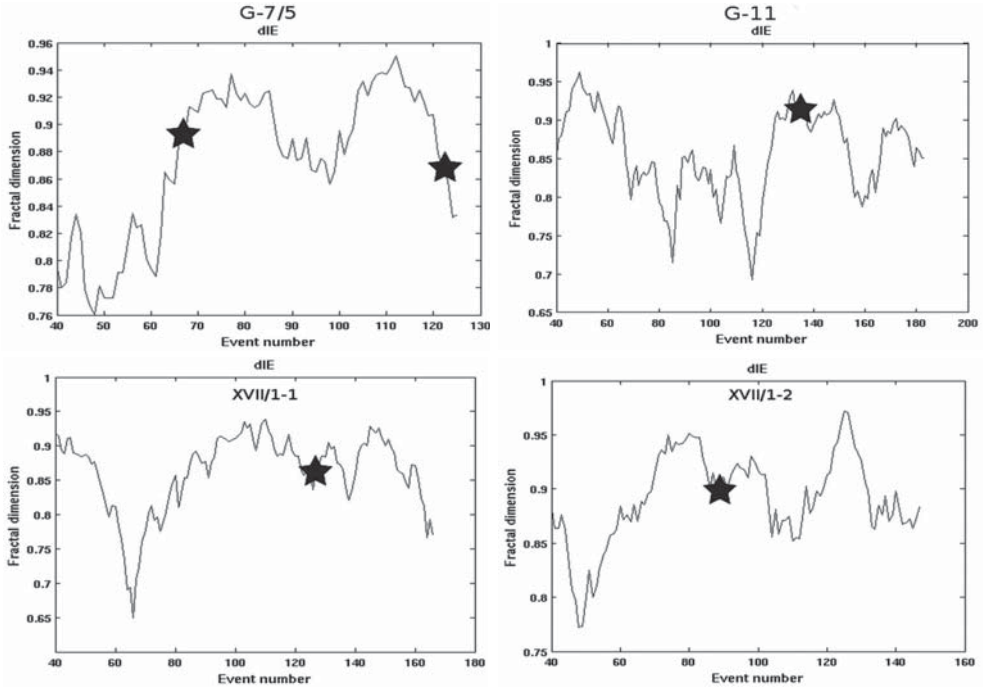

Fig. 8. Temporal changes of fractal correlation dimension of dlE parameter. The solid line represents the fractal correlation dimension and stars are the high energetic events: G7/5-1, G7/5-2 (upper left panel), G11 (upper right panel), XVII/1-1 (lower left panel), XVII/1-2 (lower right panel)

and XVII/1-2 an increase in the fractal dimension of the *dlE* parameter was observed, but the patterns of change, and magnitudes of the changes as well as the offset of the increase starting points varied. The starting point of the fractal dimension of the *dlE* parameter increase in the G7/5-1 event series was about 15 samples prior the main event, and the magnitude of the change was 0.13, but after the event the fractal dimension increase continued through 10 more samples with the magnitude of the overall increase being 0.17. In the case of the G11 event, the starting point of the *dlE* parameter of the fractal dimension increase was 20 samples before the main event, and the magnitude of the change was 0.28. The G11 event happened 2-3 samples after the increase had stopped. The starting point of the *dlE* parameter fractal dimension increase prior to the XVII/1-1 event had a 60 sample offset, and the main event happened about 15 samples after the fractal dimension of *dlE* had reached the maximum value. In case of the XVII/1-2 event, the starting point of the *dlE* parameter of the fractal dimension increase offset was 40 samples and the main event happened 5 samples after the increase had reached its maximum and had started to decrease. The increase in amplitude was 0.18. Temporal behavior of the *dlE* fractal dimension before the G7/5-2 event was different. The increase in the fractal dimension of the *dlE* parameter started about 25 samples before the main event and reached a maximum value of 10 events before the main one (magnitude of change was 0.1) then the decrease started. The decrease amplitude reached 0.08 when the G7/5-2 event happened.

The final sample analyzed in terms of temporal fractal dimension changes in *ED* space was the *lE* parameter space (Fig. 9). The fractal dimension increase of the *lE* parameter before the G7/5-1, G11 and XVII/1-1 event was observed. The starting point of the increase was observed over 15, 40 and 25 events prior to the G7/5-1, G11 and XVII/1-1 events, and the value of the increase was 0.08, 0.2 and 0.27 respectively. In the case of the G7/5-1 event, the fractal dimension of the *lE* parameter drops slightly just after the event, but the overall trend of increase was then continued. The increase reached a maximum with the G7/5-2 event. After the G11 event the value of the fractal dimension of the *lE* parameter fluctuated around 0.88 value for next 20 samples (fluctuation amplitude was 0.05) and then decreased (magnitude of decrease 0.3). The value of the fractal dimension of the *lE* parameter after the XVII/1-1 event fluctuated around the 0.92 value, while the amplitude of fluctuations was 0.03. In case of the temporal changes, the fractal dimension of the *lE* parameter connected with the XVII/1-2 event for several fluctuations around the 0.9 value where a similar magnitude range were observed.

5. Summary

The temporal changes of the fractal dimension of the studied parameters were varied and did not follow the same pattern in the different studied events, although some similarities among the events in the temporal changes of the fractal dimension are observed.

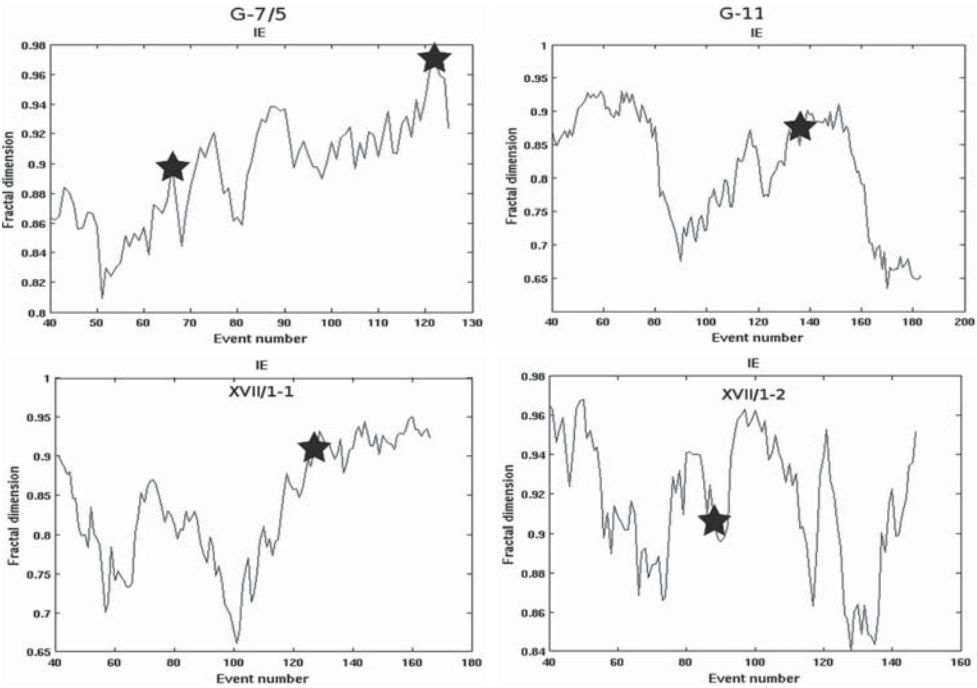

Fig. 9. Temporal changes of the fractal correlation dimension of lE parameter. The solid line represents the fractal correlation dimension and stars are the high energetic events: G7/5-1, G7/5-2 (upper left panel), G11 (upper right panel), XVII/1-1 (lower left panel), XVII/1-2 (lower right panel)

The G11 and XVII/1-1 events had common features, which are: the non double couple mechanism of event, high activity in comparison to other studied events in the considered time period and the fact that both of them were located much higher than the mining level in the anhydrite strata. The temporal variation of the fractal dimensions also show similar features for those two events. The similarity is shown in figure 7, where before a strong event, there is decrease of the fractal dimension of the *dr* parameter to a local minimum, then an increase, after which the event happened. The behavior in the temporal changes of the *dlE* and *lE* parameters for the G11 and XVII/1-1 events is shown in figures 8 and 9, and again there is a local minimum before the high energy event and the events had taken place after an increase of the fractal dimension. This means that before the XVII/1-1 and G11 events, smaller preceding events where grouped in the *dr*, *dlE* and *lE ED* parameter spaces, and after this group dispersed a high energy event happened. The fractal dimension of the *dt* before the G11 and XVII/1-1 events decreases (amplitude of decrease about 0.2), and after the event an increase of the fractal dimension can be seen (Fig. 6), but the regime of the decrease differs — in the case of G11, there is a visible and sudden drop in the fractal dimension of *dt*, whereas in the case of XVII/1-1 the main drop happens much earlier, before the event, and the main event follows a futher smaller fractal dimension drop. The interpretation of the fractal dimension drops, shortly before the main event, it can be seen that the preceding ones were clustering in the *dt* parameter space, so the interevent times became similar. They may be similarly small or large.

The third non double couple event was G7/5-2, but this event was provoked. This could have disturbed the seismogenic process before the G7/5-2 event, although there are similarities with the other two events which were observed: the decrease in the fractal dimension of the *dt* parameter before the event, and an increase in the *lE* fractal dimension before the event followed by a decrease in the fractal dimension of the *dr* parameter to a localised minimum (amplitude of decrease: 0.45, 0.2 and 0.24 respectively for XVII/1-1, G-11 and G7/5-2 events), then an increase followed by the event. The amplitude of the *lE* fractal dimension increase was about 0.17, while the other non-double couple events are characterized by a 0.2 (G11 event) and 0.27 (XVII/1-1 event) with an amplitude in the *lE* fractal dimension increasing.

The last two events — G7/5-1 and XVII-2 had some non double couple components in the mechanism solution decomposition which were observed, but the main part of the mechanism was a double couple component. The G7/5-1 was located on the excavation level and was followed by a rockburst, contrarily the XVII/1-2 event was located higher in the strata above the mining level and any effects in mining panel were not reported. Additionally the activity in the mining panels, where those events had taken place, was different. The G7/5 panel is characterized by lower activity (0.16 to 0.33 events per day) in comparison to the XVII panel (0.6 to 1.2 event per day). The increase in the fractal dimension of the *dlE* parameter and decrease of the fractal dimension of the *dt* parameter was also observed for both of the DC events as well as for all other studied events, but the pattern of the decrease differs in the events. In the case of the G7/5-1 a 0.09 decrease was observed before the event, and after the main event, the fractal dimension value fluctuated for the next 15 events and then the fractal dimension started to increase, while in the case of the XVII/1-2 event a 0.2 decrease in the fractal dimension of the *dt*

parameter was observed before the event and then the decrease continued for about 15 events (amplitude of this decrease was 0.1) and then the increase of the fractal dimension started.

The pattern in the fractal dimension temporal changes was not the same in every considered event, but a similar character of changes in the fractal dimension was observed for all events with a non double couple mechanism (G11, XVII/1-1 and G7/5-2), the most significant change was observed in the first two two events in the *dr* parameter. The third non DC event — G7/5-2 was provoked. This fact along with the event location in the ore bearing strata at mining level, while the other two were located in the upper lying anhydrite strata could explain the difference in the behavior of the studied parameters and fractal dimensions in comparison to the previous two events. The fractal dimension changes of the *lE* and *dt* parameters for all non DC events are similar — but there is an increase in the fractal dimension of the *lE* parameter before the main event and there is decrease of the *dt* fractal dimension.

The two other events (G7/5-1 and XVII/1-2) did not shown any similarity in the fractal dimension temporal variations in *dr*, *lE* parameters, although the mechanisms of the events are double couple. Only the variation of *dlE* fractal dimensions was similar — an increase before the high energetic event. The increase in the fractal dimension of the *dlE* parameter before the main event can be observed before all of the studied events, although the temporal location of the increase varied.

The main conclusions about the study may be listed:

1) A similar character of changes in the fractal dimension of *lE* and dt parameters, was observed for the events with a non double couple mechanism (G11, XVII/1-1 and G7/5-2.
2) The event which provoked G7/5-2 was blasting which is characterized by a different pattern in the fractal dimension in *dr* parameter.
3) The most significant temporal change in the fractal dimension was observed for G11, XVII/1-1 non DC events in *dr* parameter.
4) The differences in the mining situation and the source of the mechanism in the high energy events were shown in the fractal dimension of the considered ED parameters.
5) The drawback with the fractal dimension method is that the window span is limited to 30–40 events, which in some cases may be not sufficient.
6) Another weakness is that high energy event occurrence should be rare, one big event for at least 40–50 other events, because in the other cases the influence of earlier events is disturbing the fractal analysis of the later event.
7) Taking the, above mentioned drawbacks into account, the changes of the fractal dimension of the *ED* parameters, which preceded the high energy events, unveil the potential of the *ED* method in studies of interaction between events in mining induced seismicity.

The work was financed by the Ministry of Science and Higher Education under contract No. MNiSW 3935/B/T02/2010/39 during the period 2010–2012.

REFERENCES

[1] Gibowicz S.J., Kijko A.: *An Introduction to Mining Seismology.* Academic Press. San Diego 1994.
[2] Gibowicz S.J.: An Anatomy of a Seismic Sequence in a Deep Gold Mine. Pure Appl. Geophys. 150, 1997, p. 393–414.

[3] Gibowicz S.J., Lasocki S.: *Seismicity Induced by Mining: Ten Years Later.* Advances in Geophysics 44, 2001, p. 39–181.
[4] Grassberger P., Procaccia I.: *Measuring the Strangeness of Strange Attractors*. Physica D: Nonlinear Phenomena 9 (1–2): 1983, p. 189–208.
[5] Idziak A., Sagan G.., Zuberek W. M.: *The Analysis of Energy Distribution of Seismic Events from the Upper Silesian Coal Basin* [in Polish]. Publs. Inst. Geophys. Pol. Acad. Sc. M-15 (235), 1991, p. 163–182.
[6] KGHM Polska Miedź SA: http://www.kghm.pl/index.dhtml&lang=en, 20.07.2011.
[7] Kijko A.: *Keynote Lecture: Seismic Hazard Assessment in Mines.* [in:] S.J. Gibowicz and S. Lasocki (eds.). Rockbursts and Seismicity in Mines, 247–256, A.A. Balkema, Rotterdam 1997.
[8] Kijko A., Drzęźla B., Mendecki A.: *Why the Extremal Seismic Events Distribution Have the Bimodal Character?* [in Polish], Acta Montana 71, 1985, p. 225–244.
[9] Kijko A., Drzeźla B., Stankiewicz T.: *Bimodal Character of Extreme Seismic Events in Polish Mines*. Acta Geophys. Pol. 35, 1987, p. 157–166.
[10] Kijko A., Lasocki S., Graham G.: *Nonparametric Seismic Hazard Analysis in Mines.* Pure Appl. Geophys. 158: 2001, p. 1655–1676.
[11] Lasocki S.: *Non-Poissonian Structure of Mining Induced Seismicity,* Acta Montana 84, 1992, p. 51–58.
[12] Lasocki S.: *Quantitative Evidences of Complexity of Magnitude Distribution in Mining Induced Seicmicity: Implications for Hazard Evaluation*. G. van Aswegen, R. J. Durrheim and W. D. Ortlepp (eds.). The Fifth Int. Symp. on Rockbursts and Seismicity in Mines (RaSiM 5) 'Dynamic rock mass response to mining'. South African Institute of Mining and Metallurgy, Johannesburg 2001, p. 543–550.
[13] Lasocki S.: *Probabilistic Analysis of Seismic Hazard Posed by Mining Induced Events.* Controlling Seismic Risk, Proc. Sixth Int. Symp. on Rockburst and Seismicity in Mines 9–11 March 2005. Australia (Potvin, Y., Hudyma, M., eds.). Australian Centre for Geomechanics, Nedlands, 2005, p. 151–156.
[14] Lasocki S.: *Some Unique Statistical Properties of the Seismic Process in Mines.* Proceedings of the 1st Southern Hemisphere International Rock Mechanics Symp. Vol. 1: Mining and Civil, Perth, ed. Potvin, Y.. Australian Centre for Geomechanics. Nedlands, Western Australia2008, p. 667–678.
[15] Lasocki S.: *Badanie grupowania w przestrzeni parametrów tła sejsmicznego przed dużym trzęsieniem ziemi*. Geologia 35, 2009, p. 515–522.
[16] Leśniak A., Pszczoła G.: *Combined mine tremors source locations and error evaluation in the Lubin Copper Mine (Poland).* Tectonophysics, 456, 2008, p. 16–27.
[17] Lizurek G., Lasocki S.: *Badanie grupowania się zjawisk sejsmicznych indukowanych pracami górniczymi w oddziale XX-1 ZG Rudna*. Przegląd Górniczy 2012 (zaakceptowany do druku).
[18] Orlecka-Sikora B.: *The Role of Static Stress Transfer in Mining Induced Seismic Events Occurrence, a Case Study of the Rudna Mine in the Legnica-Glogow Copper District in Poland*. Geophys. J. Int. 182, 2010, p. 1087–1095.
[19] Orlecka-Sikora B., Lasocki S.: *Clustered Structure of Seismicity from the Legnica–Głogów Copper District* [in Polish]. Publs. Inst. Geophys. Pol. Acad. Sc. M-24 (340), 2002, p. 105–119.
[20] Orlecka-Sikora B., Lasocki S.: *Nonparamtric Characterization of Mining Induced Seismic Sources.* The Sixth International Symposium on Rockbursts and Seismicity in Mines "Controlling Seismic Risk" Proceedings (Y. Potvin, M. Hudyma, eds.) ACG, Perth, 2005, p. 555–560.
[21] Orlecka-Sikora B., Papadimitriou E.E., Kwiatek G.: *A Study of the Interaction Among Mining Induced Seismic Events in the Legnica–Glogow Copper District*. Poland, Acta Geophys. 57(2), 2009, p. 413–434.
[22] Trifu, C.-I., Urbancic T.I., Young R.P.: *Non-similar Frequency-magnitude Distribution for M < 1 Seismicity.* Geophys. Res. Lett. 20, 6, 1993, p. 427–430.
[23] Węglarczyk S., Lasocki S.: *A Studies of Short and Long Memory in Mining Induced Seismic Process.* Acta Geophys, 57, 2008, p. 696–715.
[24] Wiejacz P.: *Calculation of Seismic Moment Tensor for Mine Tremors from Legnica – Głogów Copper Basin*. Acta Geophys. Pol. 40, 1992, p. 103–122.